EUROPEAN ORGANIZATION FOR NUCLEAR RESEARCH

L3 Note 2599
July 21, 2000

Preliminary Standard Model Measurements at 200 GeV $< \sqrt{s} <$ 209 GeV by the L3 Experiment

The L3 Collaboration

Abstract

We summarise preliminary results of the L3 experiment obtained during the first weeks of the LEP run anno 2000 at a centre-of-mass energies between 200 GeV and 209 GeV. The total integrated luminosity analysed so far amounts to about 93 pb^{-1}. The data discussed comprise measurements of total cross sections and forward-backward asymmetries of fermion-pair production $\mathrm{e^+e^-} \rightarrow \mathrm{f\bar{f}}(\gamma)$, and of total cross sections for W-pair and Z-pair production.

Submitted to the *XXXth International Conference on High Energy Physics*
July 27 - August 2, 2000, Osaka, Japan

1 Introduction

In the year 2000 the LEP accelerator has been operated at centre-of-mass energies up to about 209 GeV, the highest energies reached with e^+e^-colliders ever, allowing to verify the Standard Model in this new energy regime. In contrast to previous years the machine was operated at many different energies. This years data has been combined in two samples with average centre-of-mass energies of 205.0 GeV and 206.8 GeV as show in Figure 1. The integrated luminosities of these event samples used in the presented analyses amount to about 59 pb^{-1} and 33 pb^{-1}, respectively.

2 Fermion-Pair production

The analysis of fermion-Pair production follows the one performed for data collected at centre-of-mass energies between 130 and 202 GeV [1–4]. Total cross sections and forward-backward asymmetries are measured for the full data samples, defined by the effective centre-of-mass energy $\sqrt{s'} > 60$ GeV for hadronic decays and $\sqrt{s'} > 75$ GeV for Z decays into muon and tau pairs (total sample), and excluding the radiative return to the Z by requiring $\sqrt{s'} > 0.85\sqrt{s}$ (high energy sample). In the Bhabha channel the samples are defined by an acollinearity cut of 120 degree and 25 degree, respectively. Figure 2 shows the distributions of the reconstructed effective centre-of-mass energies for the selected hadron, muon and tau events and of the acollinearity distribution for the selected Bhabha events.

The numbers of selected events, the preliminary cross section and forward-backward asymmetry measurements are summarised in Table 1. The errors quoted are statistical only. The cross sections and forward-backward asymmetries are shown in Figures 3, 4 and 5, where the new results are compared to our measurements at lower energies and to the Standard Model expectations as calculated using ZFITTER [5] and TOPAZ0 [6] (for $e^+e^- \to e^+e^-(\gamma)$).

3 W-pair production

The selection of $e^+e^- \to W^+W^-(\gamma)$ events follows the procedures applied for the data collected at 161 GeV and 172 GeV [7,8], 183 GeV [9] and 189 GeV [10]. The numbers of observed events in data samples are reported in Table 2. The invariant mass distributions for the qqqq and $\mathrm{qql}\nu$ final states are shown in Figure 6. Combining all decay channels we measure the total cross section $e^+e^- \to W^+W^-(\gamma)$ at 205.0 GeV to be

$$\sigma_{\mathrm{WW}} = 17.7 \pm 0.7 \pm 0.5(\mathrm{sys})\ \mathrm{pb}.$$

At 206.8 GeV our measurement is

$$\sigma_{\mathrm{WW}} = 17.2 \pm 0.9 \pm 0.5(\mathrm{sys})\ \mathrm{pb}.$$

These results are compared to our measurements at lower energies and to different Standard Model calulations in Figure 7. The theoretical cross section are calculated with the programs GENTLE [11], YFSWW3 [12] and RacoonWW [13].

4 Z–Pair Production

Events of Z–pair production are selected in the $\mathrm{q\bar{q}}\ell^+\ell^-$, $\mathrm{q\bar{q}}\nu\bar{\nu}$, $\mathrm{q\bar{q}q'\bar{q}'}$ and $\ell^+\ell^-\ell'^+\ell'^-$ final states following our previous analyses at centre–of–mass energies between 191.6 GeV and 201.7 GeV [14] and yielding the overall results listed in Table 3.

Figures 8a–c display the distributions of the variables most sensitive to the difference between signal and background for the investigated final states containing hadrons. These are the fit mass, M_{5C}, of a kinematic fit that imposes energy and momentum conservation for the production of a pair of equal mass particles in $\mathrm{q\bar{q}}\ell^+\ell^-$ events, and the outputs of two artificial neural networks for the $\mathrm{q\bar{q}}\nu\bar{\nu}$ and $\mathrm{q\bar{q}q'\bar{q}'}$ final states. The distributions comprise the full data sample. Figure 8d presents the reconstructed mass of the Z. This mass is obtained from M_{5C} for the $\mathrm{q\bar{q}}\ell^+\ell^-$ final state, from the hadronic mass after a kinematic fit that imposes the hypothesis of a Z decaying into neutrinos to the $\mathrm{q\bar{q}}\nu\bar{\nu}$ events with a high value of the neural network output, and finally from the average of the di-jet masses of the $\mathrm{q\bar{q}q'\bar{q}'}$ selected events with a high value of the neural network output.

From a binned maximum–likelihood fit to the distributions in Figures 8a–c, that takes into account also the results of the $\ell^+\ell^-\ell'^+\ell'^-$ selection, the Z–pair production cross section is measured to be:

$$\sigma_{\mathrm{ZZ}}(205.0\ \mathrm{GeV}) = 0.60^{+0.29}_{-0.30}\ \mathrm{pb} \qquad \left(\sigma^{\mathrm{SM}}_{\mathrm{ZZ}}(205.0\,\mathrm{GeV}) = 1.07\ \mathrm{pb}\right),$$

$$\sigma_{\mathrm{ZZ}}(206.8\ \mathrm{GeV}) = 0.90^{+0.40}_{-0.42}\ \mathrm{pb} \qquad \left(\sigma^{\mathrm{SM}}_{\mathrm{ZZ}}(206.8\,\mathrm{GeV}) = 1.08\ \mathrm{pb}\right).$$

The values in parentheses refer to the predictions for four–fermion final states within the Z–pair signal definition criteria [14–16] and are calculated with the EXCALIBUR [17] Monte Carlo program.

The selections of the $\mathrm{q\bar{q}}\ell^+\ell^-$ and $\mathrm{q\bar{q}}\nu\bar{\nu}$ final states are then adapted to enhance their b-quark sensitivity [14,16], already high for $\mathrm{q\bar{q}q'\bar{q}'}$ events with large values of the neural network output. The cross section for Z-pairs decaying into at least one b–pair can then be measured from the full data sample. Combining all data of this year we obtain at an average centre–of–mass energy of 205.7 GeV

$$\sigma_{\mathrm{ZZ\to b\bar{b}X}}(205.7\mathrm{GeV}) = 0.24 \pm 0.13\ \mathrm{pb} \qquad \left(\sigma^{\mathrm{SM}}_{\mathrm{ZZ\to b\bar{b}X}}(205.7\,\mathrm{GeV}) = 0.30\ \mathrm{pb}\right).$$

These cross sections are presented in Figure 9 together with the results obtained at lower centre–of–mass energies. The expected Standard Model evolution curves are also shown.

Acknowledgements

We wish to congratulate the CERN accelerator divisions for the successful upgrade of the LEP machine and to express our gratitude for the excellent performance of the machine. We acknowledge with appreciation the effort of all engineers, technicians and support staff who have participated in the construction and maintenance of this experiment.

References

[1] L3 Collab., M. Acciarri et al., Phys. Lett. **B 370** (1996) 195.

[2] L3 Collab., M. Acciarri et al., Phys. Lett. **B 407** (1997) 361.

[3] L3 Collab., M. Acciarri et al., Phys. Lett. **B 479** (2000) 101.

[4] L3 Collab., ' Preliminary L3 Results on Fermion-Pair Production in e^+e^- interactions at centre-of-mass energies from 130 GeV to 202 GeV', L3 internal note #2563, paper #529 submitted to this conference.

[5] D. Bardin et al., FORTRAN package ZFITTER, Preprint CERN-TH 6443/92;
D. Bardin et al., Z. Phys. **C 44** (1989) 493;
D. Bardin et al., Nucl. Phys. **B 351** (1991) 1;
D. Bardin et al., Phys. Lett. **B 255** (1991) 290.

[6] G. Montagna et al., Nucl. Phys. **B 401** (1993) 3;
G. Montagna et al., Comp. Phys. Comm. **76** (1993) 328.

[7] L3 Collab., M. Acciarri et al., Phys. Lett. **B 398** (1997) 223.

[8] L3 Collab., M. Acciarri et al., Phys. Lett. **B 407** (1997) 419.

[9] L3 Collab., 'Measurement of W-Pair Cross Sections and W-Decay Branching Fractions at LEP', L3 internal note #2276, paper #501 submitted to this conference.

[10] L3 Collab., 'Preliminary Results on the Measurement of W-Pair Cross Sections in e^+e^- Interactions at $\sqrt{s} = 189$ GeV and W-Decay Branching Fractions', L3 internal note #2376, paper submitted to this conference 6_253.

[11] The GENTLE version 2.0 is used.
D. Bardin et al., GENTLE/4fan v. 2.0: A Program for the Semi-Analytic Calculation of Predictions for the Process $e^+e^- \to 4f$, DESY 96-233, hep-ph/9612409.

[12] YFSWW3 version 1.14 is used.
S. Jadach et al., Phys. Rev. **D 54** (1996) 5434; Phys. Lett. **B 417** (1998) 326; Phys. Rev. **D 61** (2000) 113010; hep-ph/0007012.

[13] A. Denner et al., Phys. Lett. **B 475** (2000) 127; hep-ph/0006307.

[14] L3 Collaboration, M. Acciarri et al., ICHEP2000, contributed paper 502.

[15] L3 Collab., M. Acciarri et al., Phys. Lett. **B 450** (1999) 281.

[16] L3 Collab., M. Acciarri et al., Phys. Lett. **B 465** (1999) 363.

[17] R. Kleiss and R. Pittau, Comp. Phys. Comm. **83** (1994) 141;
see also F.A. Berends, R. Kleiss and R. Pittau in "Physics at LEP2", CERN 96-01, Vol. 2, eds. G. Altarelli, T. Sjöstrand and F. Zwirner.

$\sqrt{s} = 205.0$ GeV	total sample			high energy sample		
	# events	σ [pb]	A_{FB}	# events	σ [pb]	A_{FB}
$\mathrm{e^+e^-} \rightarrow$ hadrons(γ)	4595	81.1 ± 1.2	–	1242	19.2 ± 0.5	–
$\mathrm{e^+e^-} \rightarrow \mu^+\mu^-(\gamma)$	197	5.7 ± 0.5	0.50 ± 0.15	99	2.5 ± 0.3	0.49 ± 0.08
$\mathrm{e^+e^-} \rightarrow \tau^+\tau^-(\gamma)$	146	6.1 ± 0.9	0.35 ± 0.09	87	2.6 ± 0.3	0.60 ± 0.10
$\mathrm{e^+e^-} \rightarrow \mathrm{e^+e^-}(\gamma)$	1200	21.2 ± 0.6	0.756 ± 0.019	1094	19.4 ± 0.6	0.781 ± 0.017

$\sqrt{s} = 206.8$ GeV	total sample			high energy sample		
	# events	σ [pb]	A_{FB}	# events	σ [pb]	A_{FB}
$\mathrm{e^+e^-} \rightarrow$ hadrons(γ)	2422	76.8 ± 1.6	–	641	17.5 ± 0.7	–
$\mathrm{e^+e^-} \rightarrow \mu^+\mu^-(\gamma)$	50	4.6 ± 0.9	0.62 ± 0.33	23	1.7 ± 0.5	0.73 ± 0.28
$\mathrm{e^+e^-} \rightarrow \tau^+\tau^-(\gamma)$	76	5.6 ± 0.8	0.37 ± 0.15	37	2.0 ± 0.4	0.61 ± 0.21
$\mathrm{e^+e^-} \rightarrow \mathrm{e^+e^-}(\gamma)$	660	21.1 ± 0.8	–	605	19.4 ± 0.8	–

Table 1: Results on fermion-pair production at $\sqrt{s} = 205.0$ GeV and $\sqrt{s} = 206.8$ GeV. The number of events selected in the data, the measured cross sections (σ) and forward-backward asymmetries (A_{FB}) are listed for the total and the high energy event samples. For the Bhabha asymmetry measurement both event samples have been combined.

	205.0 GeV	206.8 GeV
$\mathrm{e^+e^-} \rightarrow \mathrm{W^+W^-}$	# events	# events
$\rightarrow \mathrm{qq\,e}\nu$	123	67
$\rightarrow \mathrm{qq}\,\mu\nu$	118	67
$\rightarrow \mathrm{qq}\,\tau\nu$	106	52
$\rightarrow \ell\nu\,\ell\nu$	69	27
$\rightarrow$ qqqq	524	279
Total	940	492

Table 2: Number of selected W-pair events for the different decay channels at $\sqrt{s} = 205.0$ GeV and 206.8 GeV.

Channel	Data Events	ZZ Signal MC	Background MC
$\mathrm{q\bar{q}}\ell^+\ell^-$	7	7.3	1.9
$\mathrm{q\bar{q}}\nu\bar{\nu}$	131	12.9	115.5
$\mathrm{q\bar{q}q'\bar{q}'}$	239	30.9	210.9
$\ell^+\ell^-\ell'^+\ell'^-$	0	0.5	0.4

Table 3: Number of observed data and expected ZZ and background Monte Carlo events.

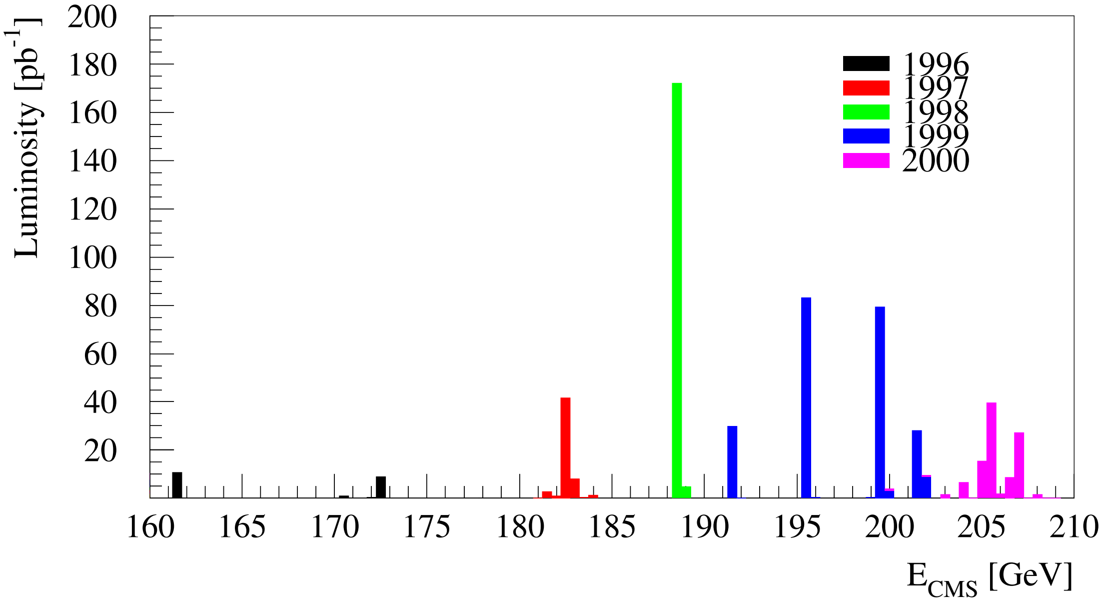

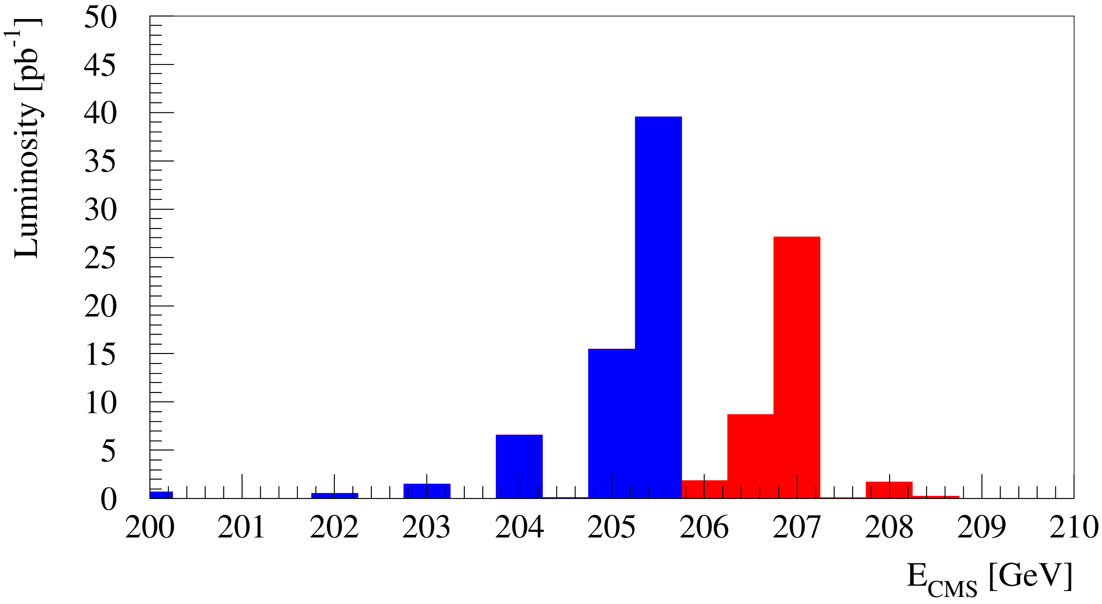

Figure 1: Distributions of the integrated luminosity as recorded by the L3 experiment. The upper plot shows all data above the W-Pair threshold, the lower plot shows this years data and how it is combined for the analyses presented in the paper.

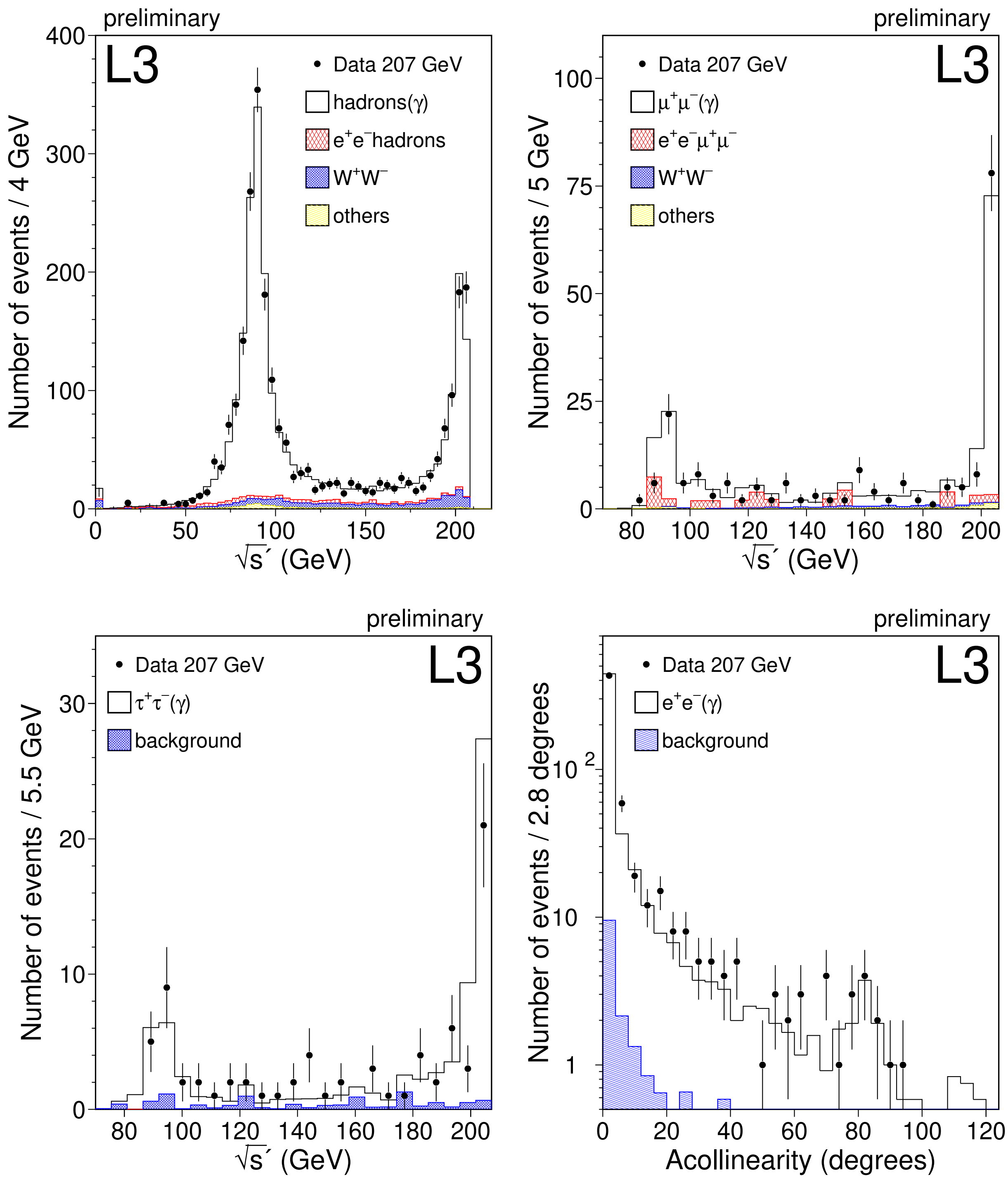

Figure 2: The reconstructed effective centre–of–mass energy, $\sqrt{s'}$, for the selection of (a) $e^+e^- \rightarrow$ hadrons(γ) events, (b) $e^+e^- \rightarrow \mu^+\mu^-(\gamma)$ events, (c) $e^+e^- \rightarrow \tau^+\tau^-(\gamma)$ events and the acollinearity angle, ζ, for (d) $e^+e^- \rightarrow e^+e^-(\gamma)$ events at centre-of-mass energies greater than 205.5 GeV.

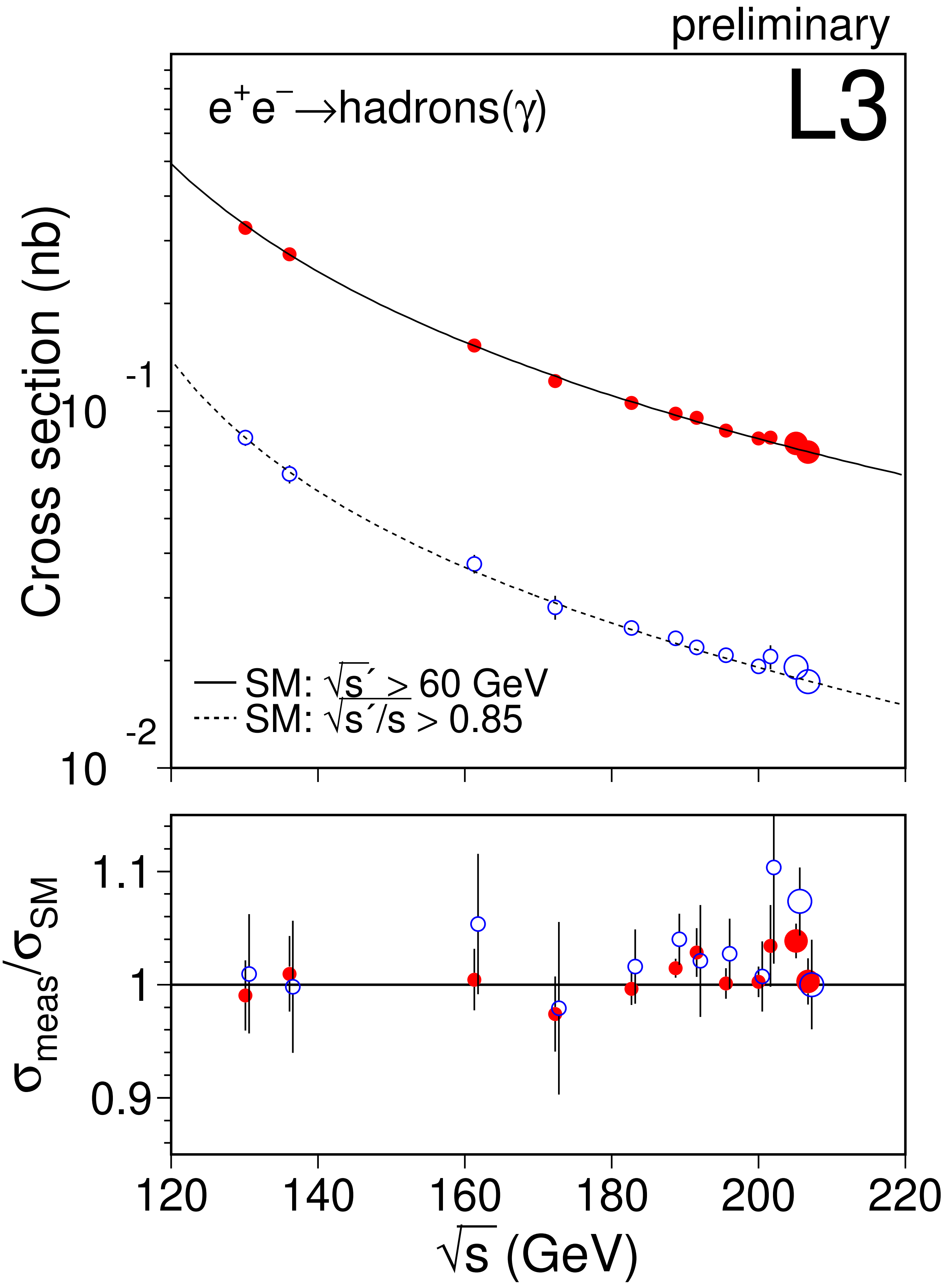

Figure 3: Measured cross sections of the reaction $e^+e^- \to$ hadrons(γ) as function of the centre-of-mass energy.

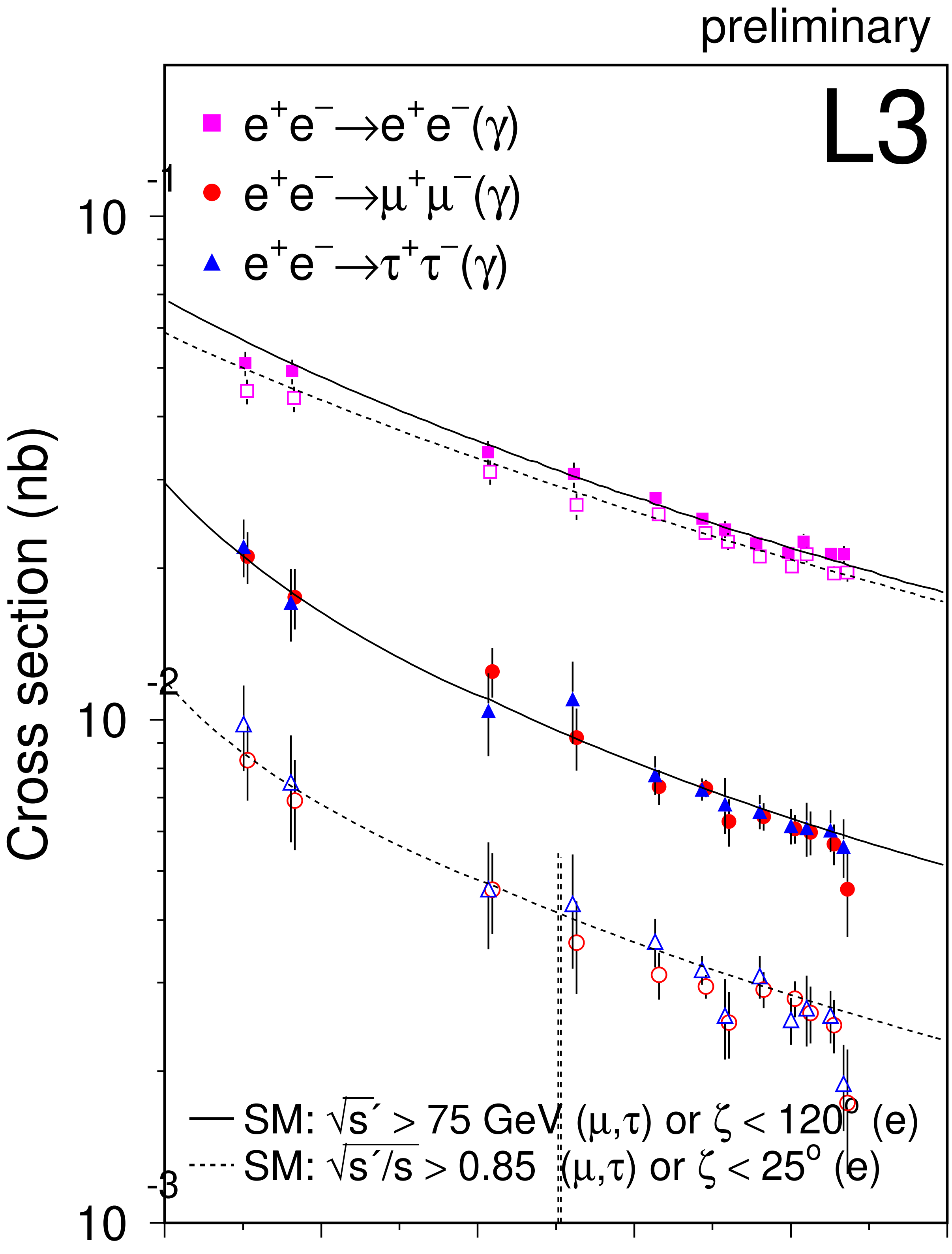

Figure 4: Measured cross sections of the reactions $e^+e^- \rightarrow \mu^+\mu^-(\gamma)$, $e^+e^- \rightarrow \tau^+\tau^-(\gamma)$ and $e^+e^- \rightarrow e^+e^-(\gamma)$ as function of the centre-of-mass energy. The results for muon- and tau-pair production have been combined.

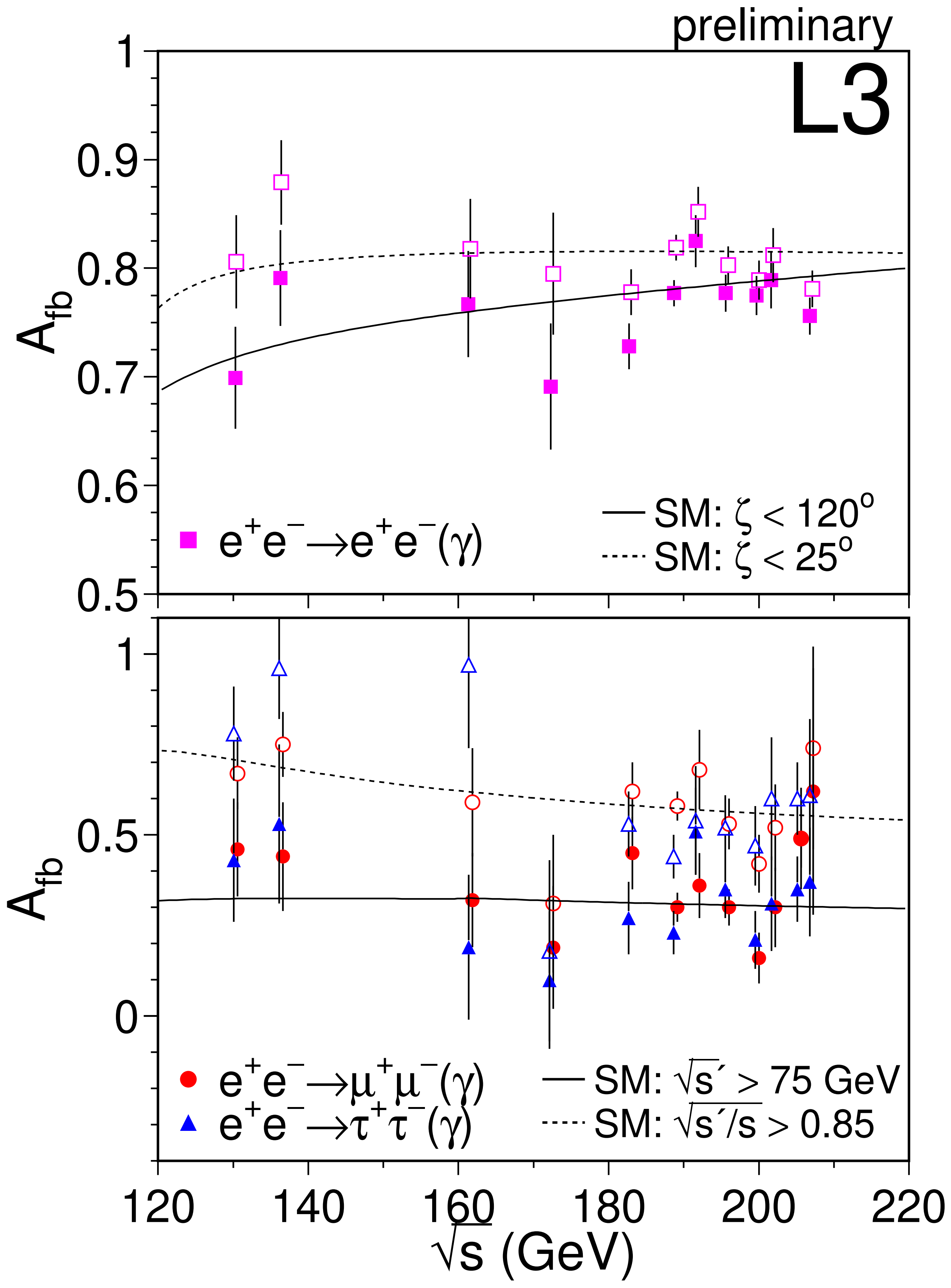

Figure 5: Measured forward-backward asymmetries of the reactions $e^+e^- \to \mu^+\mu^-(\gamma)$, $e^+e^- \to \tau^+\tau^-(\gamma)$ and $e^+e^- \to e^+e^-(\gamma)$ as function of the centre-of-mass energy. The results for muon- and tau-pair production have been combined.

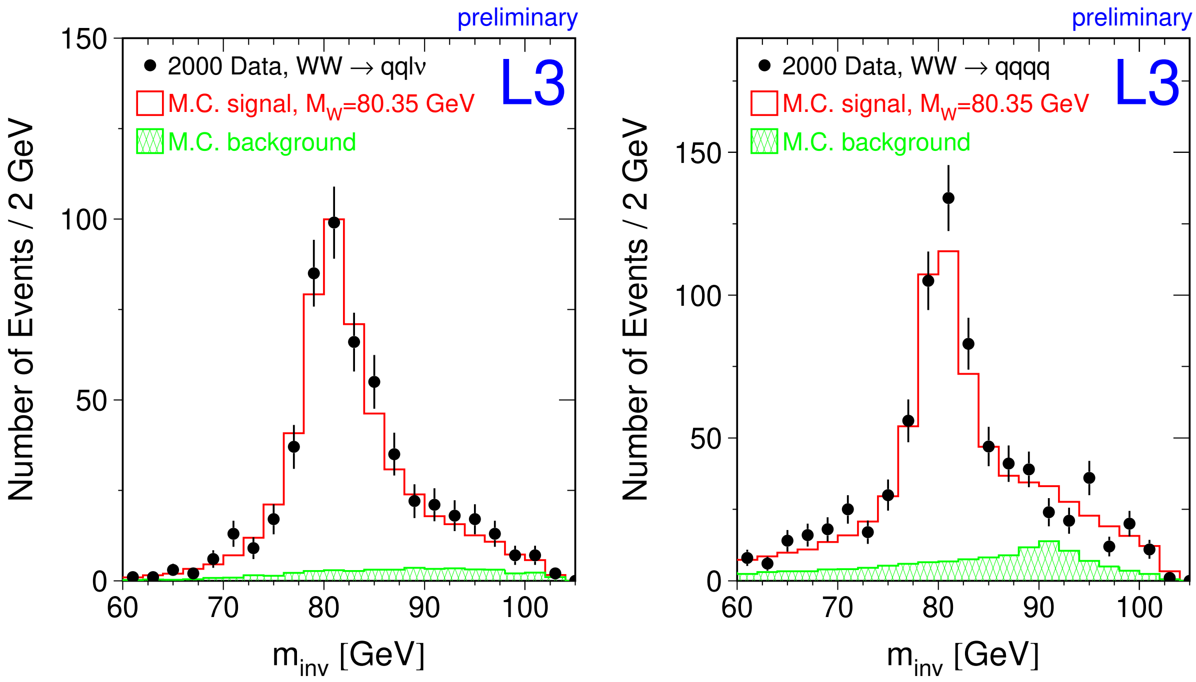

Figure 6: Invariant mass distributions for selected semileptonic and fully hadronic decays in W-pair production.

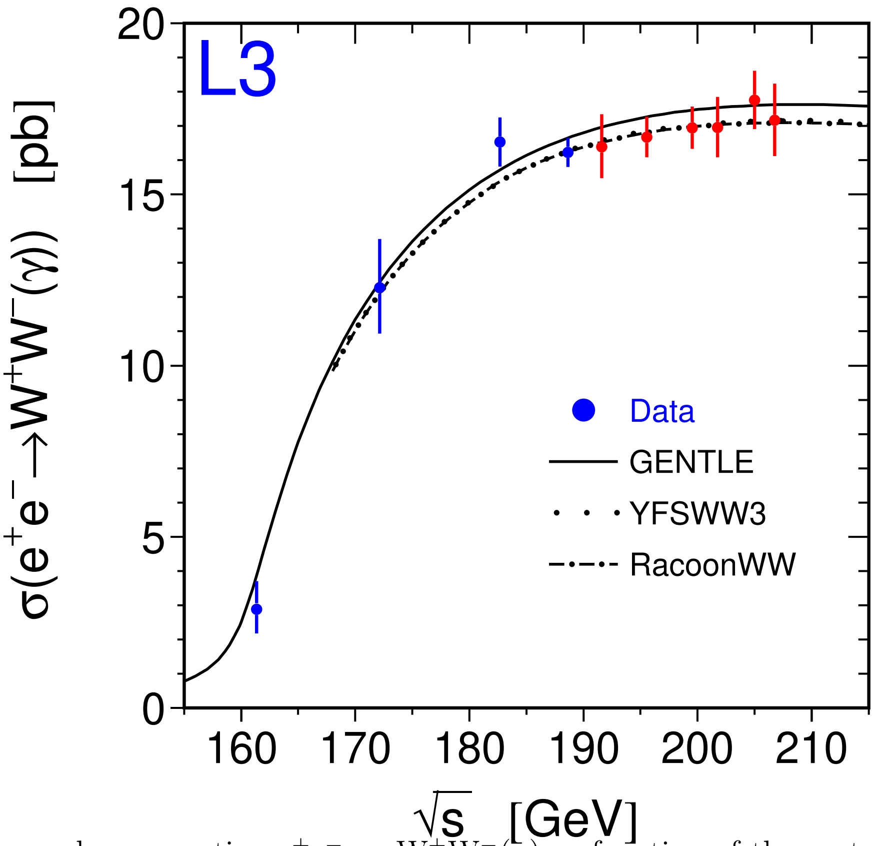

Figure 7: Measured cross section $e^+e^- \to W^+W^-(\gamma)$ as function of the centre-of-mass energy compared to various models.

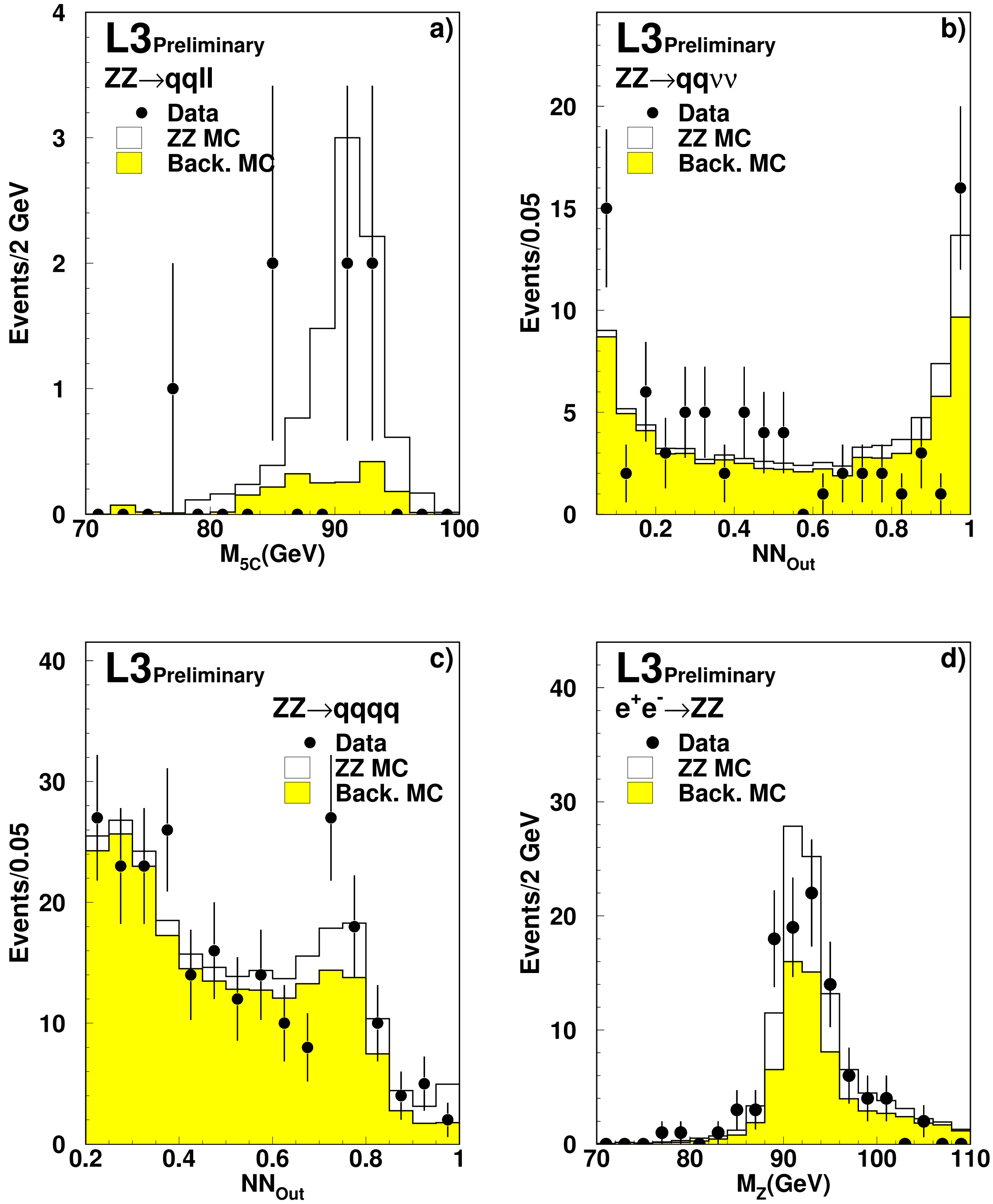

Figure 8: a) Results of a kinematic fit that imposes four momentum conservation and equal masses in the $q\bar{q}\ell^+\ell^-$ selection. Neural network outputs for the b) $q\bar{q}\nu\bar{\nu}$ and c) $q\bar{q}q'\bar{q}'$ final states. d) Reconstructed Z mass for selected events.

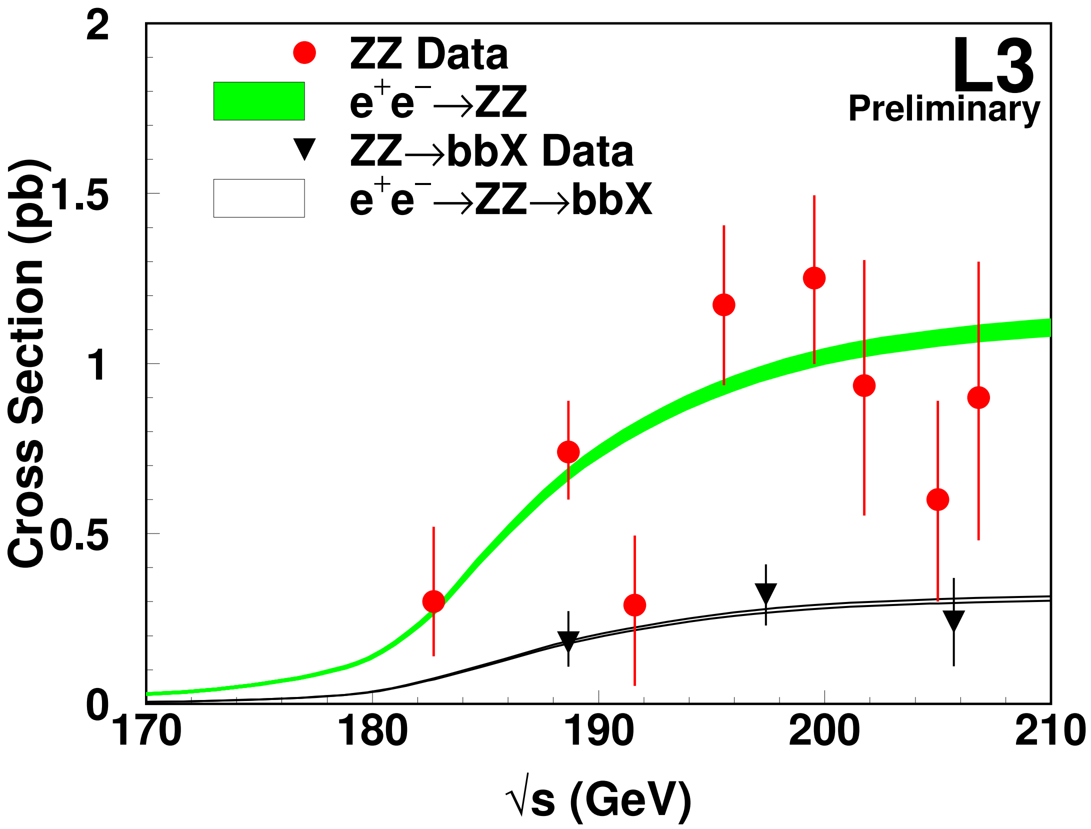

Figure 9: Standard Model predictions for the ZZ and ZZ $\rightarrow b\bar{b}X$ cross sections and the corresponding measurements. Signal definition cuts are applied and a 2% uncertainty is associated to the predictions.